

Supporting Online Material

Materials and Methods

NAD⁺ reporter system

NAD boxes were introduced between the *EcoRI/XbaI* sites of pHISi (Clontech) to generate pDS529 and annealed oligonucleotide sequences are available upon request. pDS529 was integrated at the *URA3* locus by linearizing with *XhoI*. *S. typhimurium nadR* was cloned from pFW38-46 into the *BamHI/XhoI* sites of pSE1107 (Clontech) to generate pDS526, which encodes a heterologous fusion of NadR, GAL4 activation domain (AD) and a nuclear localization signal. Loss-of-function mutations in *nadR* were generated by PCR mutagenesis of the NNMT core domain (1) (His77Ala) and the RNK mutant (2) was a carboxy-terminal truncation that removed the entire RNK domain from amino acids 227 - 410. *HAP4* was subcloned from pADH-HAP4 into pSP400 (3) between *NotI* sites and integrated at the *URA3* locus as per pDS526. All reporter strains were based on the parent strain NSY64. Gene disruptions were generated by a one-step kanamycin procedure. *BNA6* was disrupted in RA435 (W303-1A parent) to ensure adequate uptake of labeled nicotinic acid. In all analyses, where nicotinic levels in the media were in vast excess, this strain behaves identically to wild type with respect to *NAD⁺* levels and lifespan extension by CR (4, 5). Petite strains were generated by plating strains overnight on YPD medium with EtBr (20 mM) and rho minus status was confirmed by fluorescence microscopy of 4',6-diamidino-2-phenylindole dihydrochloride (DAPI)-stained cells. All deletion strains were confirmed by PCR or Southern blotting and expression of NadR-AD was confirmed in each transformant by Western blotting

using a polyclonal rabbit anti-Gal4-AD antibody (Santa Cruz). Reporter assay medium consisted of either 2.0% (unless otherwise stated) with either histidine (40 $\mu\text{g}/\text{ml}$) or without histidine + 3-AT (10 mM). Leucine was omitted from all reporter assay media to maintain the *LEU2*-based reporter plasmids. All assays were performed on at least three independent transformants and representative results are shown.

NMR spectroscopy

For NMR analyses, cells were harvested from G0 media (5) in mid-logarithmic growth phase ($A_{600} = 1.1$), centrifuged, washed once and suspended to a concentration of $2.5\text{-}2.9 \times 10^9$ cells/ml in 50 mM KPi (pH 7.4)/6% D_2O . NMR experiments were performed using a 10-mm NMR tube containing 3 ml of cell suspension. To avoid settling down of the cells and to ensure an adequate supply of gases to the cell suspension an air-lift system was used inside the NMR tube (6). To make the system anaerobic or aerobic, argon or air, respectively, was bubbled through the air-lift system 10 min before and continuously after acquisition was started. Spectra were acquired sequentially before and after addition of glucose (2% w/v). The intracellular levels of labeled metabolites were monitored non-invasively for 80 min using ^{13}C -NMR. $[3\text{-}^{13}\text{C}]\text{lactate}$ (0.2 mM) in a glass capillary was used as a concentration standard. Due to the fast pulsing conditions used for acquiring in vivo ^{13}C -spectra, correction factors were determined to convert peak intensities into concentrations. A cell suspension was prepared as described above for ^{13}C -NMR experiments and air was bubbled using the air-lift. Fully and partially relaxed spectra were acquired over an extended time period and the correction factor for the C5 of NAD^+ (0.67 ± 0.01) was determined as described previously (7). The quantitative kinetic data for

intracellular metabolites were calculated from the areas of the relevant resonances, by applying the correction factors and comparing with the intensity of the lactate resonance in the glass capillary. Average values derived from two independent experiments were used. The lower limit for *in vivo* NMR detection of intracellular NAD⁺ or NADH under these conditions was 0.3 mM. Intracellular metabolite concentrations were calculated using a value of 19.6 femoliters/cell of *S. cerevisiae* in mid-log phase. NMR spectra were run at 30°C with a quadruple-nucleus probe head on a Bruker DRX500 spectrometer. Acquisition of ¹³C-NMR spectra was performed as described (7), except for the number of transients (680). Carbon chemical shifts are referenced to external methanol designated at 49.3 ppm. For calculation of the correction factors and metabolite concentrations in cell extracts ¹³C-NMR spectra were acquired with a 60° flip angle and a recycle delay of 0.3 s (saturating conditions) or 60.3 s (relaxed conditions). Intracellular metabolite concentrations were calculated using a value of 19.6 femoliters/cell of *S. cerevisiae* in mid-log phase.

Enzyme assays

Recombinant GST-tagged yeast Sir2 and 6xHIS-tagged human SIRT1 were isolated from *E. coli* using standard procedures (8). A fluorescent signal is generated upon deacetylation of a histone substrate. Fluorescence was measured on a Gemini XS dual-scanning microplate spectrofluorometer (Molecular Devices) with excitation and emission wavelengths of 360 and 450 nm, respectively. Under these conditions, NADH contributed only minor fraction (< 4%) of the final fluorescence, which was subtracted in the final analysis. NADH was dissolved in water immediately prior to use. Deacetylation

assays were performed using an HDAC Fluorescent Activity Assay (BIOMOL) using H4-K12-AcK16 (Sir2) or the standard histone substrate "Fluor de Lys" (SIRT1) as previously described (9). GST-Sir2 (3 mg) or SIRT1 (20 U) were incubated with 250 mM acetylated histone substrate.

Supplemental Figure 1, Anderson et al.

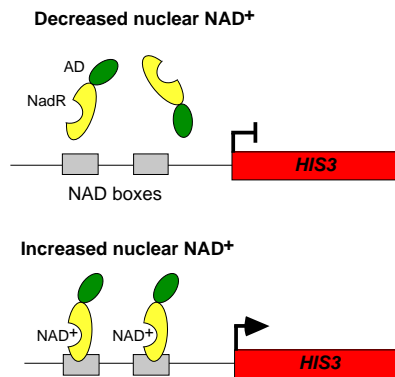


Fig. S1. In *S. typhimurium* NadR multimerizes and binds the NAD-box (TGTTTA and its inverted repeat) in a NAD⁺-dependent manner. In the yeast nucleus, the heterologous NadR-Gal4-AD fusion binds to the NAD boxes upstream of the yeast *HIS3* gene to promote growth on media lacking histidine. Leaky expression of *HIS3* is suppressed by the inhibitor 3-aminotriazole (3-AT).

Supplemental Figure 2 , Anderson et al.

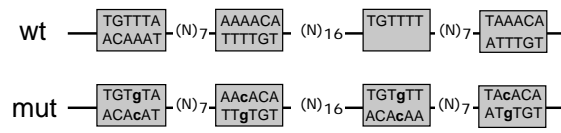


Fig. S2. Organization of NAD boxes in the reporter construct and point mutation (mut) of the consensus sequence.

Supplemental Figure 3, Anderson et al.

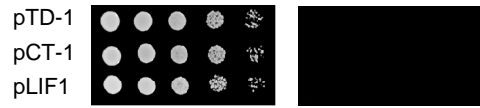


Fig. S3. Other AD fusions fail to induce expression of the *HIS3* reporter gene: pTD1, AD-SV40 large T-antigen; pCL1, Gal4 full length, pLIF1, AD-ScLif1

Supplemental Figure 4, Anderson et al.

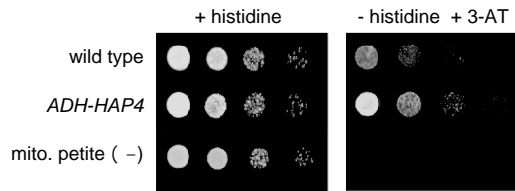


Fig. S4. The *HAP4* gene, which encodes a transcription factor that boosts respiration (10), was overexpressed in the NAD^+ reporter strain and spotted on reporter assay media. A mitochondrial petite strain with low steady state NAD^+ (-) was spotted for comparison.

Supplemental Figure 5, Anderson et al.

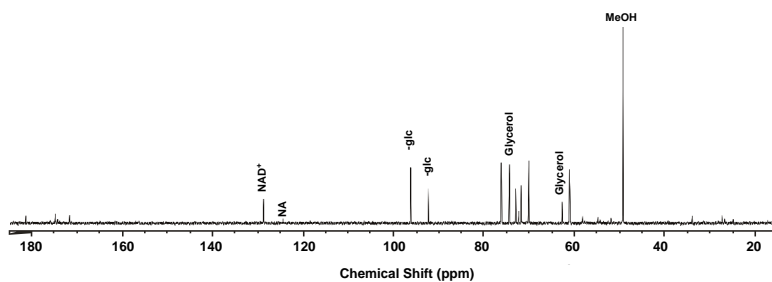


Fig. S5. Carbon spectrum of an ethanol extract obtained from *S. cerevisiae* cells growing in the presence of [5-¹³C]nicotinic acid. A single sharp line due to NAD⁺ was detected at 129.1 ppm. NADP was undetectable unless spiked into the sample (not shown). Cells were grown to an OD₆₀₀ of 0.8 in G0 medium (11) containing 2% glucose, at 30°C and 150 rpm. Methanol (2 mM) was used as a concentration standard. An intracellular concentration of 4.0 mM was found for NAD⁺. Symbols: P, polysaccharide; b-Glc, b-glucose; a-glc, a-glucose; NA, nicotinic acid; MeOH, methanol.

Supplemental Figure 6, Anderson et al.

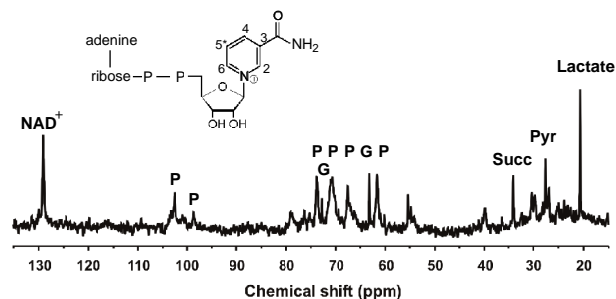


Fig. S6. *In vivo* ¹³C-NMR detection of NAD⁺. The yeast strain RA435 was grown to log-phase in defined G0 medium (11) containing 5 mg/l of [5-¹³C]nicotinic acid, then suspended in 50 mM KPi (pH 7.4) in a 10 mm NMR tube at a cell density of 2.9 x 10⁹ cells/ml and kept aerobic using an air lift system. Spectra (3.2 min acquisition, 20 Hz line broadening) were acquired sequentially before and after addition of glucose. Glucose was added to a final concentration of (2%) (w/v) at time 35.7 min after aeration was started. A ¹³C-spectrum of live cells is shown, with ¹³C-labeled C5 of the NAD⁺ nicotinamide ring indicated by an asterisk. Symbols: P, polysaccharide; G, glycerol; Succ, succinate; Pyr, pyruvate. Lactate, [3-¹³C]lactate capillary standard.

Supplemental Figure 7, Anderson et al.

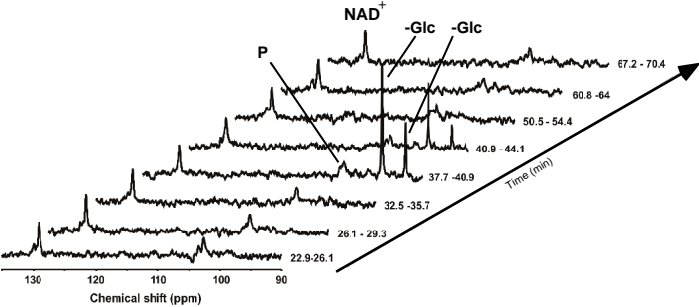


Fig.S7. A representative time-course of ^{13}C -spectra gathered for cells grown in 2.0% glucose.

References and Notes

1. N. Raffaelli *et al.*, *J Bacteriol* **181**, 5509-11 (Sep, 1999).
2. O. V. Kurnasov *et al.*, *J Bacteriol* **184**, 6906-17 (Dec, 2002).
3. B. K. Kennedy *et al.*, *Cell* **89**, 381-91. (1997).
4. S. J. Lin, P. A. Defossez, L. Guarente, *Science* **289**, 2126-8. (2000).
5. J. J. Sandmeier, I. Celic, J. D. Boeke, J. S. Smith, *Genetics* **160**, 877-89. (2002).
6. H. Santos, D. L. Turner, *J Magn Reson* **68**, 345-349 (1986).
7. A. R. Neves *et al.*, *J Biol Chem* **13**, 13 (2002).
8. J. S. Smith *et al.*, *Methods Enzymol* **353**, 282-300 (2002).
9. K. J. Bitterman, R. M. Anderson, H. Y. Cohen, M. Latorre-Esteves, D. A. Sinclair, *J Biol Chem* **277**, 45099-107. (2002).
10. S. J. Lin *et al.*, *Nature* **418**, 344-8. (2002).
11. Materials and methods are available as supporting material on *Science* Online.